Rotational bands and shape changes in ^{105}Rh

F. R. Espinoza-Quiñones, E. W. Cybulska, J. R. B. Oliveira, R. V. Ribas, M. N. Rao, M. A. Rizzutto, N. H. Medina, L. G. R. Emediato, W. A. Seale, and S. Botelho
Laboratório Pelletron, Instituto de Física, Universidade de São Paulo, São Paulo, Brazil
(Received 3 February 1997)

The ^{105}Rh nucleus has been studied by in-beam γ spectroscopy with the heavy-ion fusion-evaporation reaction ^{100}Mo(^{11}B, $\alpha 2n\gamma$) at 39 MeV. Gamma-gamma-t coincidences and directional correlation ratios were measured. Four rotational bands have been identified with similar characteristics to those in other $A\approx 100$ odd-proton nuclei. The positive-parity yrast band based on the $\pi g_{9/2}$ configuration and the negative-parity $\pi p_{1/2}$ band, showing large signature splittings, exhibit band crossings at the frequencies of 0.38 MeV and 0.48 MeV, respectively. Experimental Routhians and alignments as well as $B(M1)/B(E2)$ ratios were extracted. The structure of the bands was interpreted within the framework of the cranked shell model and total Routhian surface calculations. [S0556-2813(97)01706-8]

PACS number(s): 21.10.Re, 23.20.Lv, 25.70.Gh, 27.60.+j

I. INTRODUCTION

In the $A\approx 100$ mass region, the proton Fermi level spans the upper half of the $\pi g_{9/2}$ intruder subshell as Z increases from 40 to 50. Over this range, the γ-deformation tendencies of this relatively high-j shell vary smoothly from triaxial collective to prolate noncollective forms [1], while the β_2 deformation decreases from about 0.3 to nearly 0. On the other hand, the neutron Fermi level ($N\approx 60$) lies below or near the bottom of the $\nu h_{11/2}$ high-j shell with a driving force towards $\gamma \geqslant 0°$. The normal-parity quasiparticle states in this region originate from the $\pi(p_{1/2}, p_{3/2}, f_{5/2})$ and $\nu(g_{7/2}, d_{5/2})$ subshells, which do not modify significantly the γ deformations. The equilibrium deformation of the nucleus will depend on the interplay of the driving forces when two or more high-j quasiparticles are involved. The $\pi g_{9/2}$ bands in the odd Rh and Ag isotopes (with proton Fermi level in the middle of the subshell) show large signature splitting. When one or two $h_{11/2}$ quasineutrons are coupled to that configuration, resulting in two-quasiparticle (odd-odd ^{102,104}Rh [2] and ^{106,108}Ag [3,4] nuclei) and three-quasiparticle bands (^{103}Rh [5] and ^{105,107}Ag [3,6,7]), respectively, the signature splitting is either small or disappears and the $B(M1)/B(E2)$ ratios become relatively large. This could indicate a transition from triaxial to prolate collective shape [8]. Another type of band, with no signature splitting and very large $B(M1)/B(E2)$ ratios, has been observed also in this mass region. The interpretation for these bands is usually given by assuming a high-K configuration, which contains two $g_{9/2}$ quasiprotons, e.g., ^{109}Cd [9], ^{103}Rh [5], and ^{107,108}Ag [4,10]. An accurate description of this type of bands [11] falls beyond the scope of the standard total Routhian surface (TRS) predictions and cranked shell model (CSM) and will not be attempted here.

The nuclear structure of the ^{105}Rh nucleus is very interesting to study, because it should present many of the abovementioned phenomena. However, it is a very difficult nucleus to be produced in a fusion evaporation reaction, because it lies on the neutron-rich side of the stability line and is therefore hindered by a lack of suitable target-projectile combinations. Previous to the present work, the only information on the structure of this nucleus was based on the β-decay measuremnts in ^{105}Ru [12], particle transfer reactions [13], and an unpublished work with the ^{96}Zr(^{12}C, $p2n\gamma$) reaction [14], in which several positive-parity levels with spin up to $17/2\hbar$ were suggested, but no γ-ray transitions were reported. The spin of the ground state is known to be $7/2^+$ with the configuration of $\pi g_{9/2}$, while the configuration of the $1/2^-$ isomeric state is of a $\pi p_{1/2}$ parentage [12]. In this work, we present the results of an investigation of ^{105}Rh with ^{100}Mo(^{11}B,$\alpha 2n\gamma$) reaction as a by-product of ^{108}Ag [4]. Four rotational bands were identified in ^{105}Rh and they resemble closely those seen in ^{103}Rh [5].

II. EXPERIMENTAL PROCEDURE

High-spin states of ^{105}Rh were populated by the ^{100}Mo(^{11}B, $\alpha 2n\gamma$) reaction at 39 MeV beam energy. The beam was provided by the Pelletron accelerator of the University of São Paulo. The target used was ≈ 20 mg/cm^2 metallic self-supporting foil of enriched ^{100}Mo. The γ-ray measurements included excitation functions, γ-γ-t coincidences, and directional correlation (DCO) ratios. The coincidence data were obtained with two Compton-suppressed HPGe detectors placed at $\pm 50°$ and two HPGe detectors at $\pm 140°$, and a multiplicity filter composed of eight NaI(Tl) detectors was placed above and below the target. These data were gain matched and sorted into two-dimensional arrays. A symmetrized $E_\gamma \times E_\gamma$ matrix was constructed containing about 70×10^6 coincident events and the analysis of data was performed using the PANORAMIX code [15]. In order to obtain the multipolarities of the γ transitions using the DCO method, separate $E_\gamma(\pm 50°)\times E_\gamma(\pm 140°)$ matrices were also constructed and the analyses of data were performed using the VAXPAK codes [16]. A $E_\gamma \times t$ matrix was used to search for delayed γ rays in a 20–500 ns time interval. The symmetrized $E_\gamma \times E_\gamma$ matrix was used to establish the level scheme of ^{105}Rh. Background-subtracted gate spectra were generated from this matrix. Examples of spectra constructed from the sum of gates are shown in Fig. 1. The γ-ray tran-

 © 1997 The American Physical Society

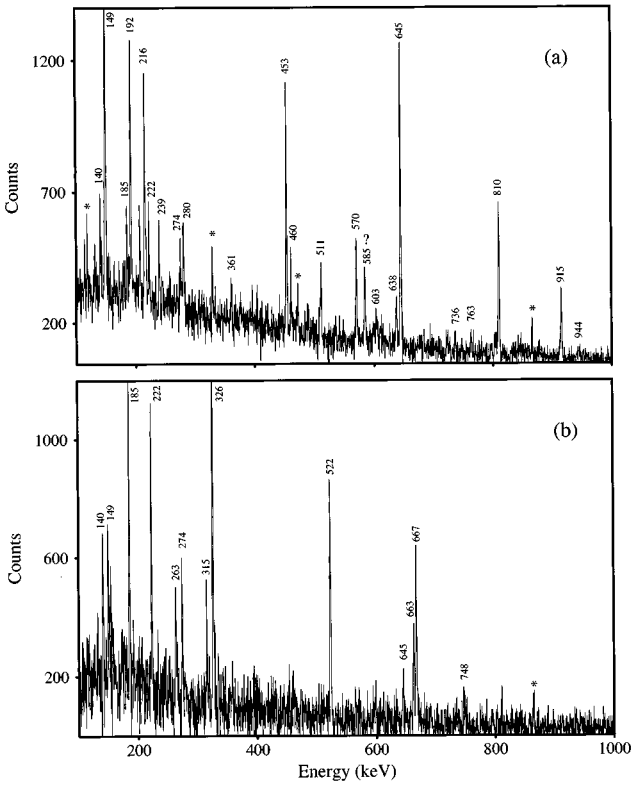

FIG. 1. Sum of background-subtracted γ-γ-coincidence spectra of the ^{100}Mo(^{11}B,$\alpha 2n$)^{105}Rh reaction at 39 MeV showing transitions in positive- and negative-parity bands. The spectra in (a) and (b) were constructed from the sum of gates on the 149.2-, 453.3-, 645.3-, 809.9-, and 914.8-keV γ rays and from 140.4-, 185.2-, 326.1-, 522.4-, 667.6-, and 662.9-keV γ rays, respectively. The (*) indicate known contaminants from the ^{107,108}Ag nuclei; question marks are for unplaced γ rays.

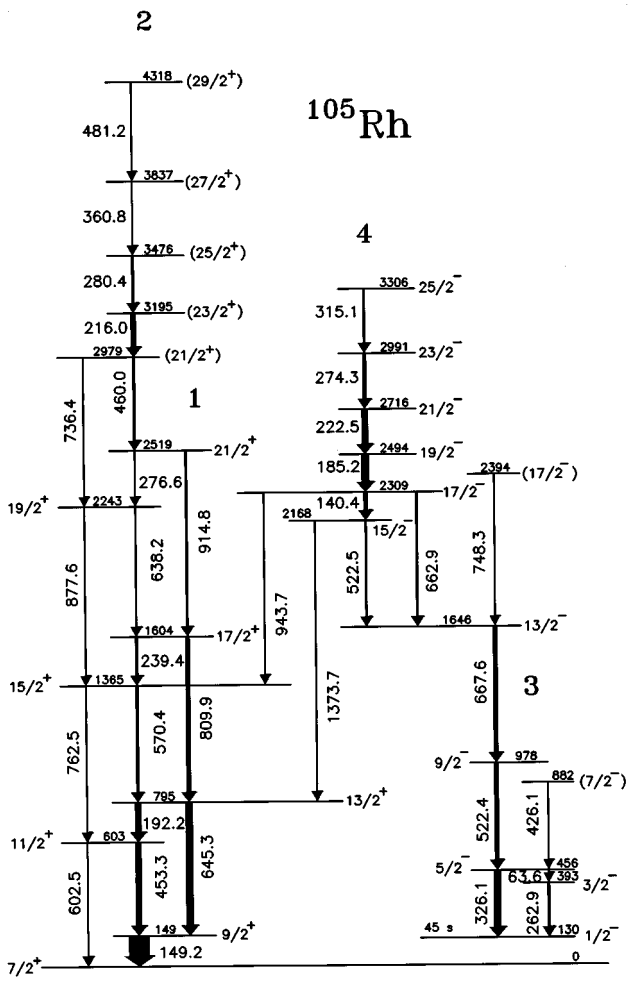

FIG. 2. The level scheme of ^{105}Rh obtained from the ^{100}Mo (^{11}B,$\alpha 2n\gamma$) reaction at 39 MeV.

sitions belonging to ^{105}Rh were identified by setting gates on the known 149.2 and 326.1 keV γ rays [13]. The DCOQ ratios are referred to a quadrupole transition gate and reflect the multipolarity of coincident γ rays. The sum of gates on several quadrupole transitions was used in order to determine the DCOQ ratios of weak γ-ray transitions. The theoretical DCOQ ratios are 1.0 if the transitions involved are of the quadrupole character. For $\Delta I=1$ transitions, the DCOQ ratios are less than 0.85. It should be noted that $\Delta I=0$ transitions could give DCOQ ratios between 0.81 and 1.03 for large mixing ratios.

III. EXPERIMENTAL RESULTS

The level scheme of ^{105}Rh, shown in Fig. 2, was constructed up to $I^{\pi}=(29/2^+)$ at an excitation energy of 4318 keV on the basis of the γ-γ coincidence relations, considering intensity-energy balances. The energies and the relative intensities for all γ-ray transitions assigned to ^{105}Rh were extracted from coincidence spectra and are listed in Table I. The table also contains the level energies with their proposed spins and parities, as well as the measured DCOQ ratios. The observed levels are grouped into four structures with rotational band characteristics, labeled 1–4 for purposes of discussion. In the present study, the bands based on the $7/2^+$ ground state (band 1) and on the $1/2^-$ isomeric state at 130 keV level (band 3) were confirmed and extended to $I^{\pi}=21/2^+$ and $I^{\pi}=17/2^-$, respectively. Furthermore, two new sidebands (2 and 4) were observed and are firmly established by the γ-γ coincidences, as shown in Fig. 1. The yrast, positive-parity band (band 1) shows the $E2$ transitions slightly stronger than the $M1$ below the band crossing, but above it (band 2) only the $M1$ transitions were observed. The negative-parity band (band 3), however, is characterized by strong $E2$ and very weak or unobserved $M1$ transitions. At higher energies and spins, band 3 is strongly fed by band 4 which presents similar characteristics to band 2.

The assignment of spins and parities in bands 1, 3, and 4 was based on the DCO ratios, rotational band characteristics, and the systematics of odd-Z nuclei in this mass region. In the case of band 2, the positive parity was corroborated by the CSM calculations (see Sec. IV), while the $\Delta I=1$ sequence of spins based on the $(21/2^+)$, 2979 keV level was chosen mainly on the basis of a close similarity with the ^{103}Rh nucleus [5]. However, this choice is not a unique one, since a sequence of spins 23/2, 25/2, 27/2, 29/2, and 31/2 is also possible.

The experimental Routhians (e') and alignments (i) for the four bands in ^{105}Rh as a function of the rotational frequency ($\hbar\omega$) are shown in Fig. 3 and were calculated fol-

TABLE I. Energies, spin assignments, relative intensities (I_γ), and DCOQ ratios (R_{DCOQ}) for the γ-ray transitions in the ^{100}Mo(^{11}B,$\alpha 2n$)^{105}Rh reaction at 39 MeV. The γ-ray energies are accurate to $\pm$ 0.3 keV. E_i and E_f are the energies of the initial and final states corresponding to each transition.

E_γ [keV]	E_i [keV]	E_f [keV]	$I_i^\pi \rightarrow I_f^\pi$	I_γ	R_{DCOQ}
63.6	455.7	392.5	$5/2^- \rightarrow 3/2^-$	2.4(8)	
140.4	2308.6	2168.1	$17/2^- \rightarrow 15/2^-$	19.9(15)	0.7(2)
149.2	149.2	0.0	$9/2^+ \rightarrow 7/2^+$	100.0(12)	0.7(1)
185.2	2493.8	2308.6	$19/2^- \rightarrow 17/2^-$	37.6(13)	0.8(2)
192.2	794.5	602.5	$13/2^+ \rightarrow 11/2^+$	31.7(13)	0.7(2)
216.0	3195.4	2979.4	$(23/2^+) \rightarrow (21/2^+)$	26.1(15)	
222.5	2716.3	2493.8	$21/2^- \rightarrow 19/2^-$	32.5(15)	0.8(1)
239.4	1604.4	1364.9	$17/2^+ \rightarrow 15/2^+$	14.8(12)	
262.9	392.5	129.6	$3/2^- \rightarrow 1/2^-$	13.3(15)	0.6(2)
274.3	2990.6	2716.3	$23/2^- \rightarrow 21/2^-$	19.0(12)	0.7(3)
276.6	2519.4	2242.6	$21/2^+ \rightarrow 19/2^+$	3.1(12)	
280.4	3475.8	3195.4	$25/2^+ \rightarrow 23/2^+$	13.9(12)	
315.1	3305.7	2990.6	$25/2^- \rightarrow 23/2^-$	11.1(10)	
326.1	455.7	129.6	$5/2^- \rightarrow 1/2^-$	36.2(9)	1.1(1)
360.8	3836.6	3475.8	$(27/2^+) \rightarrow (25/2^+)$	7.6(7)	
426.1	881.8	455.7	$7/2^- \rightarrow 5/2^-$	2.4(5)	
453.3	602.5	149.2	$11/2^+ \rightarrow 9/2^+$	29.3(7)	0.7(2)
460.0	2979.4	2519.4	$(21/2^+) \rightarrow 21/2^+$	14.4(7)	
481.2	4317.8	3836.6	$(29/2^+) \rightarrow (27/2^+)$	<1.0	
522.4	978.1	455.7	$9/2^- \rightarrow 5/2^-$	21.4(24)	1.0(1)
522.5	2168.1	1645.7	$15/2^- \rightarrow 13/2^-$	9.6(10)	
570.4	1364.9	794.5	$15/2^+ \rightarrow 13/2^+$	15.1(10)	0.7(2)
602.5	602.5	0.0	$11/2^+ \rightarrow 7/2^+$	7.0(9)	
638.2	2242.6	1604.4	$19/2^+ \rightarrow 17/2^+$	8.1(24)	
645.3	794.5	149.2	$13/2^+ \rightarrow 9/2^+$	34.6(10)	1.0(1)
662.9	2308.6	1645.7	$17/2^- \rightarrow 13/2^-$	12.3(14)	1.0(1)
667.6	1645.7	978.1	$13/2^- \rightarrow 9/2^-$	20.8(9)	1.0(1)
736.4	2979.4	2242.6	$21/2^+ \rightarrow 19/2^+$	3.1(4)	
748.3	2394.0	1645.7	$(17/2^-) \rightarrow 13/2^-$	4.5(15)	0.9(3)
762.5	1364.9	602.5	$15/2^+ \rightarrow 11/2^+$	5.7(7)	
809.9	1604.4	794.5	$17/2^+ \rightarrow 13/2^+$	20.4(9)	1.0(2)
877.6	2242.6	1364.9	$19/2^+ \rightarrow 15/2^+$	3.1(6)	
914.8	2519.2	1604.4	$21/2^+ \rightarrow 17/2^+$	10.5(6)	1.0(3)
943.7	2308.6	1364.9	$17/2^- \rightarrow 15/2^+$	2.8(6)	
1373.7	2168.1	794.5	$15/2^- \rightarrow 13/2^+$	2.8(4)	

lowing the procedure described in [17,18] with Harris parameters of $\mathcal{J}_0 = 4\hbar^2$ MeV^{-1} and $\mathcal{J}_1 = 40\hbar^4$ MeV^{-3} taken from ^{102}Ru [19]. The low-lying collective bands 1 and 3 show a large signature splitting ($\Delta e' \approx$ 200 keV) and an alignment of about $3\hbar$ and $2\hbar$, respectively. Around the frequencies of 0.40 MeV and 0.48 MeV, a band crossing is observed in bands 1 and 3, respectively. Above these crossings, bands 2 and 4 exhibit a gain in alignment of $8\hbar$ and 5 $\hbar$ relative to bands 1 and 3, respectively, an absence of signature splitting, and enhancement of $M1$ transitions.

Experimental ratios of reduced transition probabilities $[B(M1)/B(E2)]$ are indicators of the deformation parameters γ and β_2 and can also give insight into the structure of the band. All the experimental data for these ratios were obtained from the spectra gated by the transitions populating the level of interest. The experimental $B(M1)/B(E2)$ ratios for band 1 in ^{105}Rh are shown in Fig. 4, together with the lower and upper limits for bands 2, 4, and 3, respectively, as well as the theoretical estimates using the geometrical model of Dönau and Frauendorf [18].

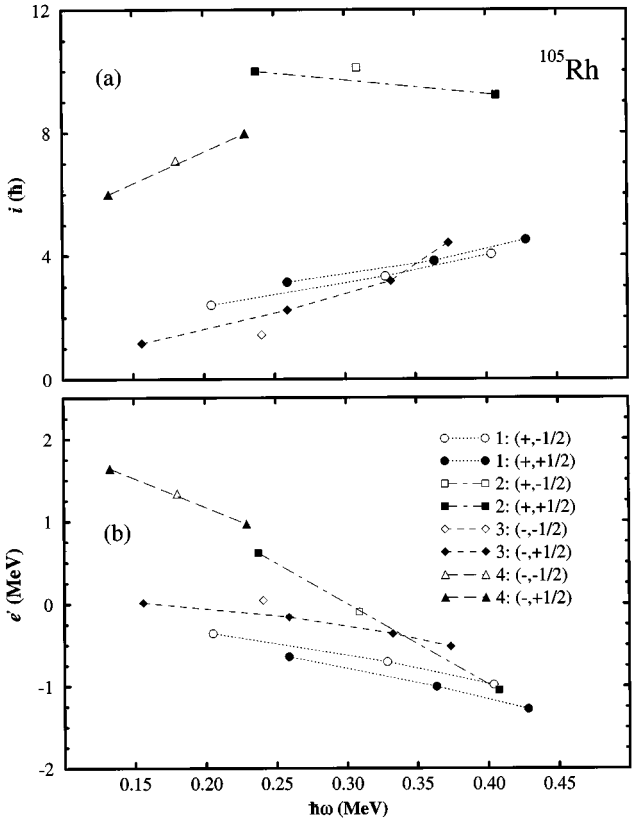

FIG. 3. Experimental quasiparticle (a) alignments and (b) Routhians as a function of the rotational frequency $\hbar\omega$ for the rotational bands labeled 1–4 in ^{105}Rh. The solid symbols correspond to $\alpha = +\frac{1}{2}$ and the open ones to $\alpha = -\frac{1}{2}$. The following symbols are used for the bands: circles, band 1; squares, band 2; diamonds, band 3; and triangles, band 4.

IV. THEORETICAL CALCULATIONS

A. CSM calculations

The quasiparticle Routhians, calculated with the cranked shell model, based on a deformed Woods-Saxon potential including pairing interactions [20] are shown in Fig. 5. The calculations were performed for $Z=45$ ($\beta_2=0.19$, $\beta_4=0.0$, $\gamma=-30°$) and $N=60$ ($\beta_2=0.19$, $\beta_4=0.0$, $\gamma=0°$) at fixed deformations, which were indicated by the TRS predictions for the $\pi g_{9/2}$ and $\pi g_{9/2} \otimes (\nu h_{11/2})^2$ configurations in ^{105}Rh. The various quasiparticle states are classified by parity and signature (π, α) and the slopes of the trajectories are directly related to the aligned angular momentum (i). In order to simplify notation a letter code was used. For the protons, the first available $g_{9/2}$ orbitals are labeled by lower case letters a, b, c, d, e, and f, and the $\pi p_{1/2}$ orbitals are labeled by g and h, while, for the neutrons, the first available $h_{11/2}$ orbitals are A, B, C, and D, and for $\nu g_{7/2}$ and $\nu d_{5/2}$ orbitals are E, F, and G, H, respectively.

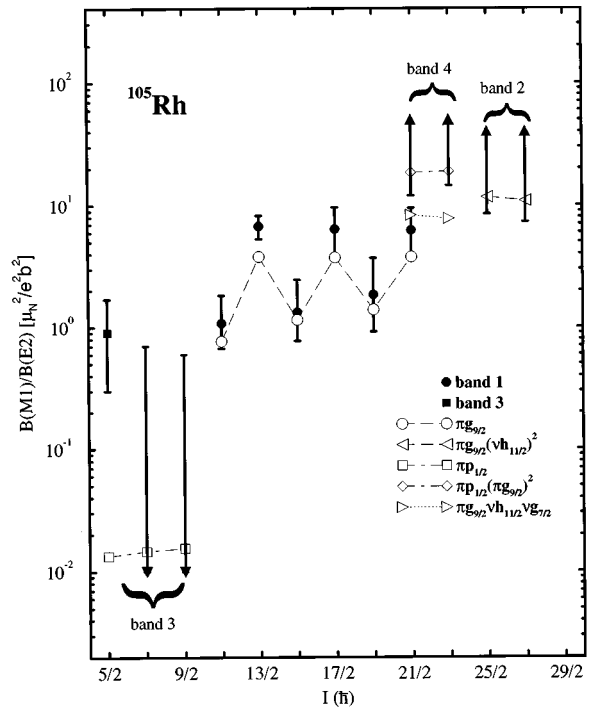

FIG. 4. Reduced transition probabilities in ^{105}Rh. The experimental $B(M1)/B(E2)$ ratios are given by solid symbols: circles, band 1; and squares, band 3, and upper or lower limits, shown for some levels in bands 2, 3, and 4 in ^{105}Rh. Calculated values are given by open symbols connected by dashed, dotted, and dot-dashed lines. The estimates were made using the equilibrium deformation $\beta_2 = 0.19$, $\beta_4 = 0$, $\gamma = -30°$, and $K = 7/2$ for $\pi g_{9/2}$ bands (circles). For the remaining bands the deformation parameters $\beta_2 = 0.19$, $\beta_4 = 0$, $\gamma = 0°$ and $K = 7/2$, 1/2 , 17/2, and 7/2 were assumed for $\pi g_{9/2} \otimes (\nu h_{11/2})^2$ (left-pointing triangles), $\pi p_{1/2}$ (squares), $\pi p_{1/2} \otimes (\pi g_{9/2})^2$ (diamonds), and $\pi g_{9/2} \otimes \nu(h_{11/2}, g_{7/2})$ (right-pointing triangles) configurations, respectively.

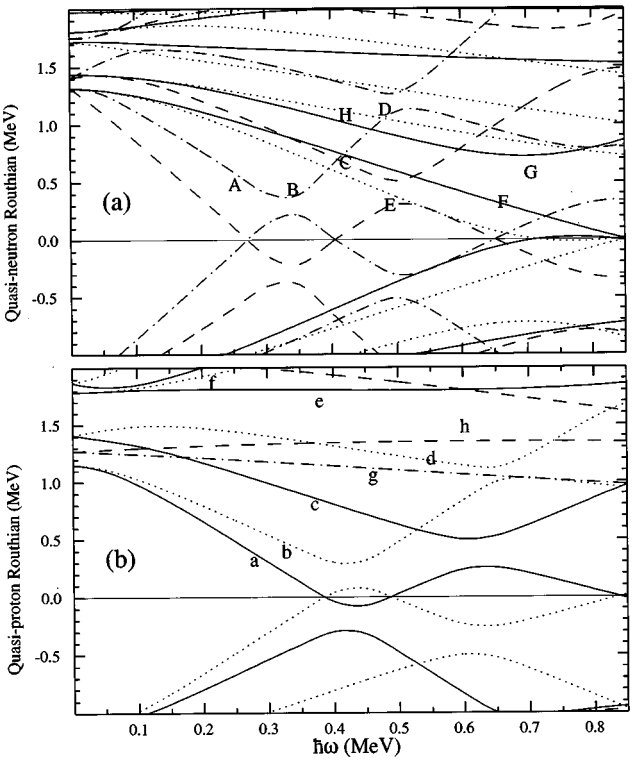

FIG. 5. Quasiparticle Routhians as a function of rotational frequency for neutrons (a) calculated at $\beta_2 = 0.19$, $\beta_4 = 0$, $\gamma = 0°$ and protons (b) calculated at $\beta_2 = 0.19$, $\beta_4 = 0$, $\gamma = -30°$ in ^{105}Rh. The following convention is used for the levels: solid line ($\pi = +, \alpha = +\frac{1}{2}$), dotted line ($\pi = +, \alpha = -\frac{1}{2}$), dot-dashed line ($\pi = -, \alpha = +\frac{1}{2}$), and dashed line ($\pi = -, \alpha = -\frac{1}{2}$). The configurations are labeled by letters.

The lowest available one-quasiproton excitations correspond to a and b ($\pi g_{9/2}$) configurations, which show a large energy splitting and are assigned to the two signature branches of the yrast band (band 1). The first two negative-parity quasiproton excitations (g, h) are an admixture of $p_{1/2}$, $f_{5/2}$, and $p_{3/2}$ and also have a large signature splitting, where the g $(-,\frac{1}{2})$ configuration corresponds to the favored $E2$ stretched cascade (band 3). Bands with these configurations have been previously observed in other odd-Z nuclei of this mass region. Moreover, as the rotational frequency increases, a band crossing of the yrast band is observed around $\hbar\omega = 0.40$ MeV and corresponds to the alignment of the first two $h_{11/2}$ quasineutrons (A and B), resulting in a net gain in angular momentum of about $10\hbar$. The next band crossing corresponds to the breaking of the first $g_{9/2}$ quasiproton pair (ab) and would occur around $\hbar\omega = 0.43$ MeV, but is blocked in the yrast band (a and b configurations).

B. TRS calculations

Total Routhian surface calculations were performed in order to get a quantitative estimate of the equilibrium deformation and to follow the nuclear shape evolution, as a function of the rotational frequency. The calculations employed the Strutinsky shell-correction formalism, deformed Woods-Saxon potential, and a monopole pairing residual interaction [20,21]. The nucleus ^{105}Rh is very γ soft and its energy minimum is very shallow below the band crossing, extending toward oblate-collective deformations, as shown in Fig. 6. There is a strong indication for configuration-dependent triaxiality in the one-quasiproton configurations $g_{9/2}$ [Fig. 6(a)] and $p_{1/2}$ [Fig. 6(c)].

The result for yrast configuration a ($\pi g_{9/2}$) at $\hbar\omega = 0.317$ MeV is shown in Fig. 6(a). For this configuration, a very large negative γ deformation ($\gamma \approx -30°$) and a large signature splitting (250 keV at $\hbar\omega \approx 0.32$ MeV) are predicted below $\hbar\omega = 0.4$ MeV. The signature splitting of 250 keV is close to that extracted from band 1. Above this frequency, the three-quasiparticle configuration containing two $h_{11/2}$ quasineutron (aAB) becomes yrast, with a resulting prolate-collective shape ($\gamma \approx 0°$), as shown in Fig. 6(b). This configuration is predicted to have a small signature splitting (≈ 50 keV at $\hbar\omega \approx 0.45$ MeV), comparable to the experimental value for band 2. The γ-deformation change from triaxial- to prolate-collective shape is due to the strong driving force of the $(\nu h_{11/2})^2$ quasineutrons, which also results in an alignment gain of $10\hbar$. Since $h_{11/2}$ quasineutrons dominate the nuclear shape ($\gamma \approx 0°$) and the energy splitting of the $g_{9/2}$ quasiproton tends to zero around $\gamma = 0°$, the small signature splitting ($\approx$ 50 keV) of the three-quasiparticle configuration is essentially between the a and b quasiproton states.

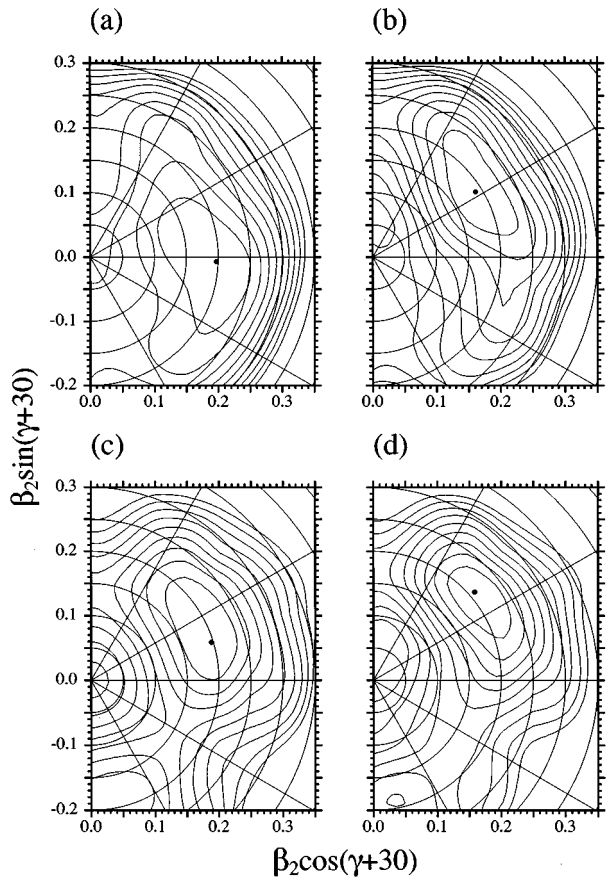

FIG. 6. Total Routhian surface calculations for one- and three-quasiparticle configurations in ^{105}Rh. (a) a configuration, $\hbar\omega=0.317$ MeV; minimum at $\beta_2=0.197$, $\beta_4=0.008$, $\gamma=-32°$. (b) aAB configuration, $\hbar\omega=0.444$ MeV; minimum at $\beta_2=0.190$, $\beta_4=0.009$, $\gamma=2.2°$. (c) g configuration, $\hbar\omega=0.317$ MeV; minimum at $\beta_2=0.197$, $\beta_4=0.010$, $\gamma=-12.6°$. (d) gAB configuration, $\hbar\omega=0.444$ MeV; minimum at $\beta_2=0.210$, $\beta_4=0.009$, $\gamma=9.3°$ (the thick dots indicate the position of the equilibrium deformation).

The situation is similar when examining the g $(\pi p_{1/2})$ configuration. The equilibrium deformation remains almost unchanged at a triaxial-collective shape ($\gamma\approx-12°$) for frequencies below $\hbar\omega=0.40$ MeV, as shown in Fig. 6(c). Around $\hbar\omega=0.30$ MeV the energy splitting between the favored (g) and unfavored (h) signatures is $\approx$180 keV, which is close to that observed for band 3. As a consequence of the additional strong driving forces of the AB pair, the energy minimum is pulled towards positive γ values ($\gamma\approx10°$) for the gAB configuration, as shown in Fig. 6(d). Such a deformation change does not affect significantly the signature splitting value corresponding to the $\pi p_{1/2}$ configuration. At $\hbar\omega=0.381$ MeV, this value is around 300 keV for the $\pi p_{1/2}\otimes(\nu h_{11/2})^2$ configuration, which is in complete disagreement with that for band 4.

C. Estimated branching ratios $B(M1)/B(E2)$

In the semiclassical model of Dönau and Frauendorf [18], the $M1$ transitions are assumed to originate from the precession of the perpendicular component of the magnetic moment around the total angular momentum vector. Using this approach the branching ratios $B(M1)/B(E2)$, between in-band $\Delta I=1$ and crossover $\Delta I=2$ transitions from each band state, were estimated for the one- and three-quasiparticle configurations of ^{105}Rh and compared with the experimental results in Fig. 4. Effective g factors were used to relate the angular momentum of each quasiparticle configuration to its magnetic moment vector and were obtained from the Schmidt estimates, with an attenuation factor of 0.7 for the spin g factors [22]. The deformation parameters used were obtained from the TRS calculations for each configuration and the proton and neutron alignments were derived from the quasiparticle Routhians in Fig. 5. In the case of the $\pi g_{9/2}$ yrast band, a $K=7/2$ projection and a correction for large experimental signature splittings (200 keV) were used, while for the $\pi g_{9/2}\otimes(\nu h_{11/2})^2$ band, the $K=7/2$ projection was assumed to come essentially from the $g_{9/2}$ quasiproton. A pair of aligned $h_{11/2}$ quasineutrons ($i\approx10\hbar$) coupled to the $g_{9/2}$ quasiproton with a relatively large K value is responsible for the enhancement of $M1$ transitions, as seen in band 2. The calculations for band 3 were performed assuming a pure $p_{1/2}$ configuration with the g factor=0.03 and $K=1/2$. In the case of a pure $p_{3/2}$ ($g=1.97$) the $B(M1)/B(E2)$ ratios would increase by a factor of about 100. For the high-K $\pi p_{1/2}\otimes(\pi g_{9/2})^2$ band (gac) with a pair of $g_{9/2}$ quasiprotons coupled to the deformation axis, large $B(M1)/B(E2)$ ratios are in agreement with the experimental lower limits for band 4. Another three-quasiparticle $\pi g_{9/2}\otimes\nu(h_{11/2},g_{7/2})$ configuration (aAE and bAE) could be considered; however, the theoretical $B(M1)/B(E2)$ ratios result in smaller values than those for the experimental lower limits for band 4.

V. DISCUSSION

Band 1 is the yrast band with strong $M1$ and $E2$ transitions. The observed large signature splitting of 200 keV, according to the CSM and TRS calculations, corresponds to the lowest one-quasiproton excitations (a and b) with a large negative γ value ($\gamma\approx-30°$). The calculated $B(M1)/B(E2)$ ratios using $\Delta e'=200$ keV and $K=7/2$ are in very good agreement with the experimental results and thus the $\pi g_{9/2}$ configuration was assigned to band 1.

The three-quasiparticle band 2 is characterized by strong $M1$ transitions and is built on the second $(21/2^+)$ state of the yrast band, as shown in Fig. 1. The difference between the two structures 1 and 2 is clearly exhibited in the rotating frame (see Fig. 3) where band 2 has negligible signature splitting and a gain in alignment of about $8\hbar$ relative to band 1. These characteristics are expected for a $\pi g_{9/2}\otimes(\nu h_{11/2})^2$ configuration (aAB and bAB). TRS and CSM calculations indicate that the first band crossing occurs around $\hbar\omega=0.40$ MeV and corresponds to an alignment of a pair of $h_{11/2}$ quasineutrons (AB). This phenomenon causes a change in γ deformation from triaxial- to prolate-collective shapes. Since the signature splitting corresponds to the splitting between the two quasiprotons (a and b), it decreases as γ increases from $-30°$ to $0°$. On the basis of the geometrical model, the enhancement of the $M1$ transitions is caused by a coherent superposition of the magnetic moments of a strongly coupled proton $(g_{9/2})$ and of the two aligned neutrons $(h_{11/2})$.

On the other hand, band 3 is characterized by strong $E2$, weak, or unobserved $M1$ transitions, and a large signa-

ture splitting (200 keV). The $\pi p_{1/2}$ configuration (g and h) is expected to have a very large signature splitting with g being the lower branch, while the other one (h) should be weakly populated and difficult to observe experimentally. These properties were also seen in other odd-Z nuclei in this mass region. TRS calculations suggest triaxial-collective shape ($\gamma \approx -12°$) and a large signature splitting (180 keV) for this configuration. In addition, at $I^{\pi}=5/2^{-}$ the experimental $B(M1)/B(E2)$ ratio is rather small (roughly $1.0\mu_N{}^2/e^2\,\mathrm{b}^2$). The theoretical $B(M1)/B(E2)$ ratio was calculated for a pure $\pi p_{1/2}$ configuration and is two orders of magnitude smaller. However, admixtures from $p_{1/2}$, $p_{3/2}$, and $f_{5/2}$ are present in the first two negative-parity quasiproton excitations (g, h), increasing the effective g factor and the quasiparticle angular momentum projection along the symmetry axis (K), resulting in larger $B(M1)/B(E2)$ ratios, comparable with the experimental ones.

The three-quasiparticle band 4 decays preferentially to band 3, around $I^{\pi}=17/2^{-}$. The experimental signature splitting in band 4 is negligible and no $E2$ crossover transitions were observed. Essentially three types of configurations were considered for this band: namely, $\pi p_{1/2}\otimes(\nu h_{11/2})^2$, $\pi g_{9/2}\otimes(\nu h_{11/2},g_{7/2})$, and $\pi p_{1/2}\otimes\pi[(g_{9/2})^2]_{K=8}$. In the first case, the coupling of the $(\nu h_{11/2})^2$ to the $\pi p_{1/2}$ configuration is expected to give a fairly large signature splitting, of the same order of magnitude as for band 3, in contradiction with the experimental results. Similar results would be obtained with any other combination of two low-lying $(h_{11/2},g_{7/2})$ quasineutrons. For the second type of configuration $\pi g_{9/2}\otimes\nu(h_{11/2},g_{7/2})$, a small signature splitting would be expected. In addition, the experimental lower limits for the $B(M1)/B(E2)$ ratios for the $21/2^{-}$ and $23/2^{-}$ levels are around $13\mu_N{}^2/e^2\,\mathrm{b}^2$ in disagreement with the theoretical results ($\approx 9\mu_N{}^2/e^2\,\mathrm{b}^2$). On the other hand, for the third configuration $\pi p_{1/2}\otimes\pi(g_{9/2})^2$, the theoretical estimates ($\approx 18\mu_N{}^2/e^2\mathrm{b}^2$) are consistent with the experimental lower limits; see Fig. 4. Furthermore, this band presents a gain in alignment of about $5\hbar$ relative to band 3, which is the expected value for $(\pi g_{9/2})^2$ quasiparticles. The large K value provides also a possible explanation for the negligible signature splitting observed experimentally [11]. It should be noted that $K\approx 8$ usually implies an isomeric state for the bandhead. However, a lifetime of less than about 20 nsec cannot be measured with the experimental setup of the present experiment. Bands with this type of configuration have been observed already in this mass region in nuclei such as odd-N ^{109}Cd [23], odd-odd ^{108}Ag [4], and odd-Z ^{103}Rh [5]. In view of the above arguments, the $\pi p_{1/2}\otimes\pi[(g_{9/2})^2]_{K=8}$ configuration was tentatively assigned to band 4.

VI. CONCLUSION

A level scheme for the states populated in a heavy-ion reaction has been proposed for the ^{105}Rh nucleus. Four rotational bands were observed, which are consistent with the systematics of the odd-Z nuclei in the $A=100$ mass region. Most of the band structures were interpreted within the framework of the CSM and TRS. Triaxial deformation could explain the large signature splitting in the one-quasiproton configurations and the absence of strong $M1$ transitions. A shape change, between the yrast and the three-quasiparticle bands, above the crossing frequency of $\hbar\omega=0.4$ MeV, occurs due to the alignment of a pair of $h_{11/2}$ quasineutrons which induce the disappearance of the signature splitting and the enhancement of $M1$ transitions. The data presently available indicate that the negative, three-quasiparticle band can be ascribed to a high-K configuration [coupling the $(\pi g_{9/2})^2$ to the $(\pi p_{1/2})$ band]. This type of high-K band appears also in other nuclei in this mass region.

ACKNOWLEDGMENTS

The authors would like to acknowledge financial support from the Brazilian Conselho Nacional de Desenvolvimento Científico e Tecnológico (CNPq).

[1] G. A. Leander, S. Frauendorf, and F. R. May, *Proceedings of the Conference on High Angular Momentum Properties of Nuclei*, Oak Ridge, 1982, edited by N. R. Johnson (Harwood, New York, 1983), p. 281.

[2] R. Duffait, A. Charvet, K. Deneffe, R. Beraud, A. Emsallem, M. Meyer, T. Ollivier, J. Treherne, A. Gizon, F. Beck, and T. Byrski, Nucl. Phys. **A454**, 143 (1986).

[3] D. Jerrestam, W. Klamra, J. Gizon, F. Lidén, L. Hildingsson, J. Kownacki, Th. Lindblad, and J. Nyberg, Nucl. Phys. **A577**, 786 (1994).

[4] F. R. Espinoza-Quiñones, E. W. Cybulska, L. G. R. Emediato, C. L. Lima, N. H. Medina, J. R. B. Oliveira, M. N. Rao, R. V. Ribas, M. A. Rizzutto, W. A. Seale, and C. Tenreiro, Phys. Rev. C **52**, 104 (1995).

[5] H. Dejbakhsh, R. P. Schmitt, and G. Mouchaty, Phys. Rev. C **37**, 621 (1988).

[6] H. J. Keller, S. Frauendorf, U. Hagemann, L. Käubler, H. Prade, and F. Stary, Nucl. Phys. **A444**, 261 (1985).

[7] D. Jerrestam, W. Klamra, J. Gizon, B. Fogelberg, S. J. Freeman, H. J. Jensen, S. Mitarai, G. Sletten, and I. Thorslund, Nucl. Phys. **A579**, 256 (1994).

[8] S. Frauendorf, in *Proceedings of the International Symposium on In-Beam Nuclear Spectroscopy*, Debrecen, edited by Z. S. Dombrádi and T. Fényes (Akadémiai Kiadó, Budapest, 1984), p. 711.

[9] S. Juutinen, R. Julin, M. Piiparinen, P. Ahonen, B. Cederwall, C. Fahlander, A. Lampinen, T. Lönnroth, A. Maj, S. Mitarai, D. Müller, J. Nyberg, P. Šimeček, M. Sugawara, I. Thorslund, S. Törmänen, A. Virtanen, and R. Wyss, Nucl. Phys. **A573**, 306 (1994).

[10] F. R. Espinoza-Quiñones, E. W. Cybulska, J. R. B. Oliveira, R. V. Ribas, N. H. Medina, M. N. Rao, M. A. Rizzutto, L. G. R. Emediato W. A. Seale, and S. Botelho, Phys. Rev. C **55**, 1548 (1997).

[11] S. Frauendorf, Nucl. Phys. **A557**, 259c (1993).

[12] R. N. Saxena, V. P. Esteves, and F. C. Zawislak, J. Phys. G **5**, 1169 (1979).

[13] *Table of Isotopes*, 7th ed., edited by C. Michael Lederer and Virginia S. Shirley (John Wiley & Sons, New York, 1978), p. 469.
[14] J. A. Grau, L. E. Samuelson, P. C. Simms, S. I. Popik, and F. A. Rickey, Bull. Am. Phys. Soc. **21**, 95 (1976).
[15] V. R. Vanin and M. Aïche, Nucl. Instrum. Methods Phys. Res. A **284**, 452 (1989).
[16] W. T. Milner, Computer codes VAXPAK, Oak Ridge National Laboratory, 1986.
[17] R. Bengtsson and S. Frauendorf, Nucl. Phys. **A237**, 139 (1979).
[18] F. Dönau and S. Frauendorf, in *Proceedings International Conference on High Spin Properties of Nuclei*, Oak Ridge, 1982, edited by N. R. Johnson, Nuclear Science Research Series Vol. 4 (Harwood, New York, 1983), p. 143.
[19] D. R. Haenni, H. Dejbakhsh, R. P. Schmitt, and G. Mouchaty, Phys. Rev. C **33**, 1543 (1986).
[20] R. Wyss, J. Nyberg, A. Johnson, R. Bengtsson, and W. Nazarewicz, Phys. Lett. B **215**, 211 (1988).
[21] W. Nazarewicz, J. Dudek, R. Bengtsson, T. Bengtsson, and I. Ragnarsson, Nucl. Phys. **A435**, 397 (1985).
[22] S. Frauendorf and F. R. May, Phys. Lett. **125B**, 245 (1983).
[23] S. Juutinen, P. Šimeč, C. Fahlander, R. Julin, J. Kumpulainen, A. Lampinen, T. Lönnroth, A. Maj, S. Mitarai, D. Müller, J. Nyberg, M. Piiparinen, M. Sugawara, I. Thorslund, S. Törmänen, and A. Virtanen, Nucl. Phys. **A577**, 727 (1994).